Available online at www.sciencedirect.com
SCIENCE DIRECT®
Marine Geology 203 (2004) 219–233
MARINE GEOLOGY
INTERNATIONAL JOURNAL OF MARINE GEOLOGY, GEOCHEMISTRY AND GEOPHYSICS
www.elsevier.com/locate/margeo

# Giant landslides, mega-tsunamis, and paleo-sea level in the Hawaiian Islands

G.M. McMurtry [a,*], P. Watts [b], G.J. Fryer [a], J.R. Smith [a], F. Imamura [c]

[a] School of Ocean and Earth Science and Technology, University of Hawaii, Honolulu, HI 96822, USA
[b] Applied Fluids Engineering, Inc., Private Mail Box #237, 5710 East 7th Street, Long Beach, CA 90803, USA
[c] Department of Tsunami Engineering, Tohoku University, Aoba 06, Sendai 980-8579, Japan

Accepted 5 September 2003

**Abstract**

Landslide tsunami simulations have advanced to the point where the tsunamigenic potential of giant submarine landslides (GSL) can be affirmed, while the subsidence history of different Hawaiian Islands is still subject to debate. We show that mega-tsunamis are a sufficient explanation for the observed pattern of debris height of calcareous marine deposits on some of the Hawaiian Islands. Further, our tsunami simulations, using the Alika GSL as example, can be used to reduce the considerable uncertainty in subsidence history of the different Hawaiian Islands, a current obstacle to interpreting the deposits from large waves. We also show that the onset of interglacials provides a probable explanation for the timing of these giant landslides over at least the last five million years. The climate change mechanism both explains the confusion with eustatic sea-level rise and provides a reasonable triggering mechanism for giant landslides from oceanic island volcanoes.


*Keywords:* landslide; tsunami; island; subsidence; sea level

## 1. Introduction

Mega-tsunamis produced by giant submarine landslides (GSL) were first proposed for Hawaii (Moore and Moore, 1984, 1988; Moore et al., 1994a) and have since been implicated globally at other oceanic islands and along the continental margins (Lènat et al., 1989; Holcomb and Searle, 1991; Nisbet and Piper, 1998; Carracedo, 1999; Elsworth and Day, 1999). The primary evidence constitutes the large, detached submarine landslide blocks and fields of smaller debris recognized by offshore surveys (Lipman et al., 1988; Moore et al., 1989, 1994b; Fig. 1), with additional evidence such as coral deposits found at high elevations that suggest giant wave impacts on land (Moore and Moore, 1984, 1988; Moore et al., 1994a). While not discounting the possibility of locally generated tsunamis, some researchers have cast doubt upon the original hypothesis of giant waves impacting Lanai and other Hawaiian Islands from flank failures of the nearby Mauna

* Corresponding author. Tel.: +1-808-9566858; Fax: +1-808-9569225.
*E-mail address:* garym@soest.hawaii.edu (G.M. McMurtry).

0025-3227/03/$ – see front matter © 2003 Elsevier B.V. All rights reserved.
doi:10.1016/S0025-3227(03)00306-2

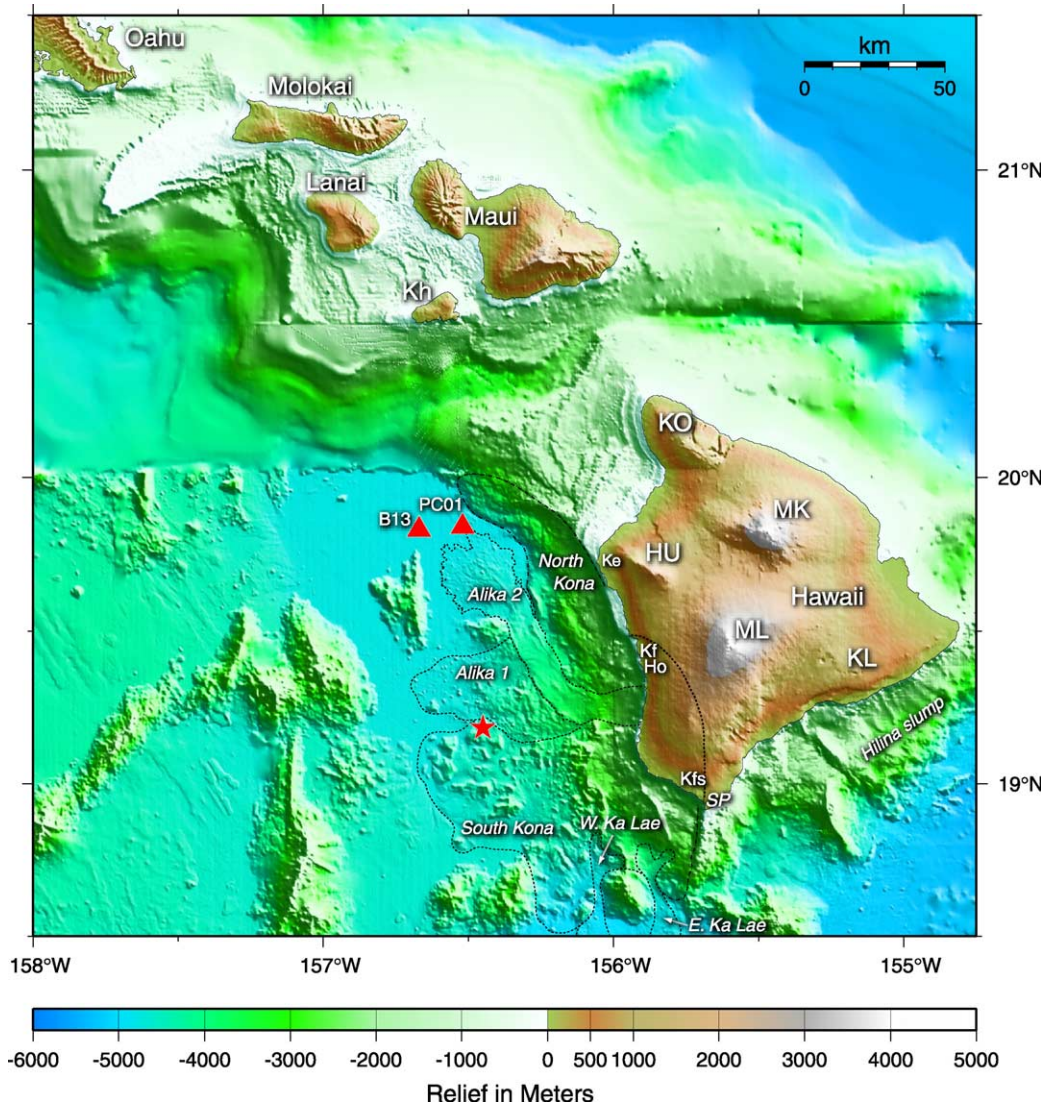


Fig. 1. Shaded relief bathymetry and topography of the southeastern Hawaiian Islands, compiled from various sources (Duennebier et al., 1994; Smith, 1994), illuminated from the northeast. The debris fields of the Alika phases 1 (thin dotted) and 2 (heavy dotted), East and West Ka Lae (thin dotted) debris avalanches, and the North and South Kona slumps are outlined (Moore et al., 1995). Also shown are the core locations used in stratigraphic dating of the Alika phase 2 (triangles; McMurtry et al., 1999) and the submersible dive location used to date the South Kona (star; Moore et al., 1995). Hawaii Island main shield volcanoes are indicated as: Mauna Loa (ML); Mauna Kea (MK); Hualalai (HU); Kohala (KO); and Kilauea (KL). The island name of Kahoolawe (Kh) and Keahole Point (Ke) on Hawaii are abbreviated. Proposed buried headwall of southwest Hawaii slide complex (Lipman, 1995) shown as heavy dotted line extending from the Kealakekua fault (Kf) to the Kahuku fault system (Kfs) near Ka Lae (South Point, SP). Hookena maximum runup location on Hawaii island (Fig. 3b) denoted by Ho.

Loa Volcano on Hawaii Island (Grigg and Jones, 1997; Felton et al., 2000; Rubin et al., 2000; Keating and Helsley, 2002). These studies have focused instead upon island uplift, complex fluvial deposition, and interglacial high stands of the sea as alternative mechanisms to explain multiple occurrences of elevated deposits from the putative tsunami waves on these islands.

Moore and Moore (1984, 1988) offered onshore evidence for a series of giant waves that swept the southwest coasts of Lanai and Kahoolawe Islands. This evidence included soil stripping to 365 m elevation on Lanai and 240 m on Kahoolawe, and thick, blanketing, chaotic deposits of basalt boulder gravels, coral fragments and calcareous beachrock slabs at lower elevations with sand and shell fragments at higher elevations (to 326 m on Lanai). Coral clasts within the 'Hulopoe Gravel' collected at 115–155 m elevation on Lanai were U-series dated at 101–134 ka (Moore and Moore, 1988). Because of its probable age and location, several researchers (Lipman et al., 1988; Moore et al., 1989; Garcia, 1996) specifically targeted the Alika GSL, phases 1 and 2, for the ca. $\geq$100-ka Lanai event (Fig. 1). Direct dating of the Alika phase 2 landslide by marine stratigraphy of its turbidite deposits indicates an age of $127 \pm 5$ ka (McMurtry et al., 1999). Similar clast-rich chaotic deposits at up to 85 m elevation on nearby Molokai Island were U-series dated at 200–240 ka (Moore et al., 1994a), and were suggested to originate from waves produced by an older event, such as the South Kona GSL that roughly corresponds to this date (Moore et al., 1995). Recently, more precise U-series dating of the coral clasts within deposits on southern Lanai, in agreement with previous dates, suggests that these deposits formed during the last two eustatic sea-level rises (stages 5e and 7, at $\sim$135 and 240 ka) (Rubin et al., 2000). Rubin et al. (2000) found evidence for significant geographical and stratigraphc ordering of the Lanai deposits, and for multiple depositional events separated by considerable time periods. They argued that this evidence invalidates the main premise of the original 'giant wave' hypothesis, namely that the coral-bearing conglomerates of the Hulopoe Gravel resulted from a rapid sequential deposition from three giant waves of a single tsunami. It is important to note, however, that their results are not inconsistent with separate depositional events from two or more mega-tsunamis of differing ages, because their dates also match known GSLs to within reasonable expected errors. We seek to explain this apparent coincidence.

## 2. Landslide modeling

In a submarine landslide, water is drawn down over the upper part of the slide and is pushed up in a broad rise over and ahead of the advancing nose. At the instant of maximum draw-down, designated the characteristic time $t_o$ by Watts (1998), the free surface above the slide is poised between draw-down and subsequent rebound. Hence, at time $t_o$, kinetic energy above the slide is near zero and potential energy is a maximum. Meanwhile, out ahead of the slide, the broad rise has been growing and expanding seaward for time $t_o$ to become the leading elevation of the seaward tsunami. Expansion of the rise means that its kinetic energy is non-zero, but for the rise too, maximum sea-surface uplift occurs at $t_o$. Overall, then, kinetic energy is a minimum and potential energy a maximum at time $t_o$. The minimum in kinetic energy means that the source of a landslide-generated tsunami can be conveniently modeled using just sea surface displacement at $t_o$ and assuming a null velocity field (Watts et al., 2003). Ignoring the kinetic energy of the initial outgoing wave must introduce some error and presumably reduces outgoing wave amplitudes, but comparison with experiments (Watts et al., 2000) and with more complete numerical treatments (Grilli et al., 2002) suggests that the errors are small.

The TOPICS tsunami source (Watts et al., 2003) is an approximation of the sea surface at time $t_o$. TOPICS has seen useful application both for slide and slump tsunami sources (Goldfinger et al., 2000; Watts et al., in press; Tappin et al., 2001). Here we shall use TOPICS to approximate the GSL tsunami source. We only simulate one GSL, Alika phase 2, because this is a test of principle, rather than an attempt at a more accurate case study for Hawaii.

The Alika 2 GSL involved most of Mauna Loa flank from the base of Hawaii Island at 4500 m water depth to at least the lower Kealakekua and Kaholo fault system near the present shoreline (Lipman et al., 1988) or the higher Kealakekua–Kahuku fault system and probable headwall (Lipman, 1995). Using the Kealakekua–Kahuku fault system as headwall, a maximum of 29% of the sliding mass was subaerial, thereby enhancing

the size of the tsunami, because most tsunami generation occurs in shallow water (Murty, 1979; Raichlen et al., 1996; Grilli and Watts, 1999). The shallow, subaerial content of the Alika 2 GSL has been verified by deposit analysis. Chemical analyses of fresh volcanic glass sampled from the turbidite immediately in front of the Alika phase 2 GSL (McMurtry et al., 1999) indicate a Mauna Loa source of primarily low S content, consistent with shallow water to subaerial deposits with some deeper (higher S) components (Dixon et al., 1991).

To describe this event, we chose a 285° slide orientation from true north, consistent with the known initial trajectory of the Alika 2 GSL submarine morphology (Fig. 1). Downslope, the landslide turned northwesterly, but such subsequent movement does not substantially affect the initial sea surface conditions that generate the tsunami, because tsunami generation is affected primarily by events in shallow water (Raichlen et al., 1996; Grilli and Watts, 1999). We used the following simplistic landslide input parameters: mean incline angle $\theta = 8°$, initial mean water depth $D = 1300$ m, initial slide length $B = 45$ km along the incline, initial maximum width $W = 20$ km, and initial maximum thickness $T = 1$ km (Fig. 2). These measurements are consistent with all known Alika 2 dimensions (Lipman et al., 1988) and match the proportions of other slides of similar geometry (Edgers and Karlsrud, 1982) despite the different slide materials involved. We need to estimate the mean density of the Alika 2 GSL. The bulk density of dry, subaerial surface flows is about 2.3 g/cm$^3$ (Kinoshita et al., 1963); for basalt within the interior of the shield, it is about 2.95 g/cm$^3$ (Ryan, 1988). We inferred a bulk slide density of $\rho_b = 2.7$ g/cm$^3$ by performing the double integral for a linear increase in density with depth along a parabolic length profile of the slide

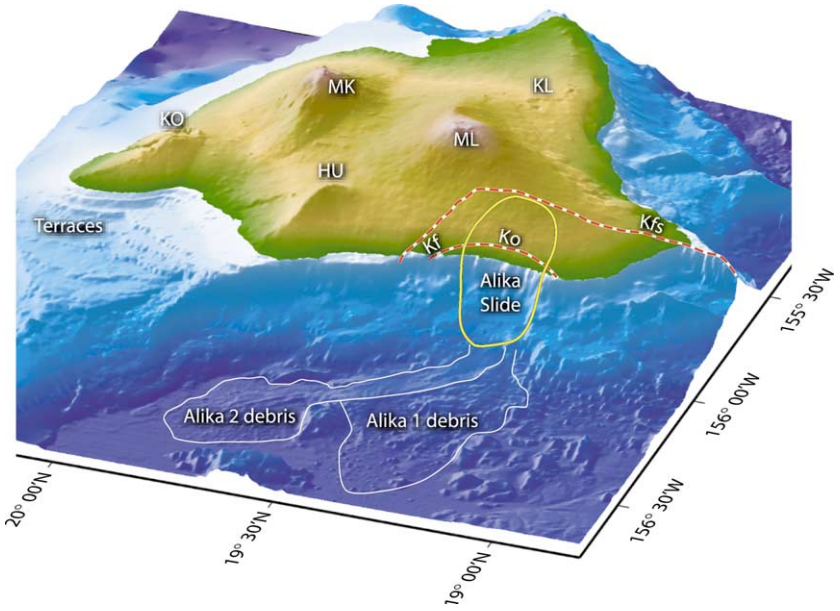


Fig. 2. Vertically exaggerated shaded relief map of the west (Kona) coast of Hawaii Island, illuminated from the west, based on the same data shown in Fig. 1, and using the same notation as for Fig. 1. An approximate outline of the maximum possible extent of the Alika GSL event is indicated by the solid yellow line, with mean incline angle $\theta = 8°$, initial mean water depth $D = 1300$ m, initial slide length $B = 45$ km along the incline, initial maximum width $W = 20$ km, and initial maximum thickness $T = 1$ km. The fault systems indicated by the Kf–Ko (lower Kealakekua and Kaholo) and Kf–Kfs (upper Kealakekua to Kahuku) red dashed lines provide lower and upper bounds on the slide headwall elevation. The debris fields of the Alika phase 1 and 2 avalanches are indicated by the solid white lines. The northward bend in the Alika phase 2 avalanche is probably too deep to influence tsunami generation. Submerged terraces off the northwest Hualalai (HU) and Kohala (KO) coasts (and also recognized off northwest Lanai) are indicated along the northern boundary of the figure.

(Fig. 2). With parabolic width and length profiles, we obtain a slide volume of around $V = 400$ km$^3$, which agrees with the *minimum* estimated volumes of the Alika event, namely 400 km$^3$ for phase 1, and 200 km$^3$ for phase 2, which probably succeeded phase 1 rapidly (Lipman et al., 1988). These input parameters complete the gross geological description needed to estimate slide motion and tsunami generation (Grilli and Watts, 1999, 2001; Goldfinger et al., 2000).

Catastrophic failure of the volcano flank is indicated by the debris deposits, which include a vast field of large, km-scale blocks nearly 100 km from the base of Hawaii Island (Lipman et al., 1988). For the slide parameters deduced above for Alika phase 2, we find that a slide initial acceleration $a_0 = 0.61$ m/s$^2$ with a characteristic duration $t_0 = 647$ s and a characteristic distance $s_0 = 257$ km using the equations of Watts (1998, 2000). The characteristic distance roughly approximates the runout distance, although part of the slide mass can travel farther as a turbidity current. Turbidite deposits of $100 \pm 20$ ka age and of mixed Mauna Loa origin believed to be from the Alika GSLs have been found 300 km west of Hawaii upon the 500-m-high Hawaiian Arch (Garcia, 1996). Based on the equations of motion given by Watts (1998, 2000), we estimate that the speed of the center of the slide when it reached the bottom of the incline at the base of the island was 170 m/s, while the speed of the head of the slide (which was subaerial before the motion) was 220 m/s at the base of the island slope. Watts and Grilli (2003) have shown that these equations of motion apply to a deforming landslide center of mass motion.

Similar landslide speeds were obtained by Fryer and Watts (2002) as well as Fryer et al. (2004) for the Ugamak GSL of similar length and volume, because maximum speed scales with the square root of landslide length (Watts and Grilli, 2003). The phase speed of a tsunami (or its celerity) in water $H = 5000$ m deep, is $\sqrt{Hg} = 220$ m/s. This velocity match between slide and tsunami means that, as the slide accelerated down the slope, it remained 'in phase' with the tsunami it was generating, building it up to exceptionally large size (Tinti and Bortolucci, 2000; Fryer and Watts, 2002; Fryer et al., 2004). Such phase coupling is captured automatically by our initial condition because it is included in the underlying modeling of Grilli and Watts (1999, 2001). Given such efficient coupling between landslide motion and wave generation, the tsunami amplitude must have been a significant fraction of the 3200 m vertical slide displacement (Murty, 1979; Watts, 1998).

The Alika 2 tsunami source after $t_0 = 647$ s of landslide motion and tsunami generation is shown in Fig. 3a. The characteristic wavelength,

$$\lambda \approx t_0\sqrt{Dg} = 73 \text{ km} \tag{1}$$

determines the source region for long wave (i.e. tsunami) propagation (Watts, 1998, 2000). The size and extent of the sea-surface displacement is proportional to the characteristic wavelength both along and transverse to the axis of failure (Watts et al., 2003). Based on our input parameters, we predict an initial depression of $-750$ m over the landslide and an initial elevation of 190 m in front of the landslide. These amplitudes result from curve fits to numerical wave tank experiments (Grilli and Watts, 1999, 2001). To show that they are not unreasonable, in 2-D the characteristic tsunami amplitude, $\eta$ is approximately:

$$\eta \approx \frac{0.218 T \sin^{1.38}\theta B^{1.25} W}{D^{1.25}(W + \lambda)} = 259 \text{ m} \tag{2}$$

(Grilli and Watts, 1999; Goldfinger et al., 2000; Watts et al., in press). Because the initial condition is derived from analytical curve fits similar to Eq. 2, a sensitivity analysis can be made using partial derivatives. The sensitivity analysis will enable error estimates to be made. From Eq. 2, amplitude is most sensitive to the incline angle $\theta$, mean depth $D$, and slide length $B$. A 1% reduction in initial width $W$ causes only a 0.79% reduction in amplitude. From such an analysis, we can explore the dependence of tsunami size on slide parameters, essentially an error estimate based on geological uncertainty. For example, adjusting depth $D$ and length $B$ to put the head scarp at the ocean surface (Fig. 2) would generate tsunami amplitudes 55% of the current tsunami source. Geological uncertainty (especially the initial landslide length and mean depth) indicates that our

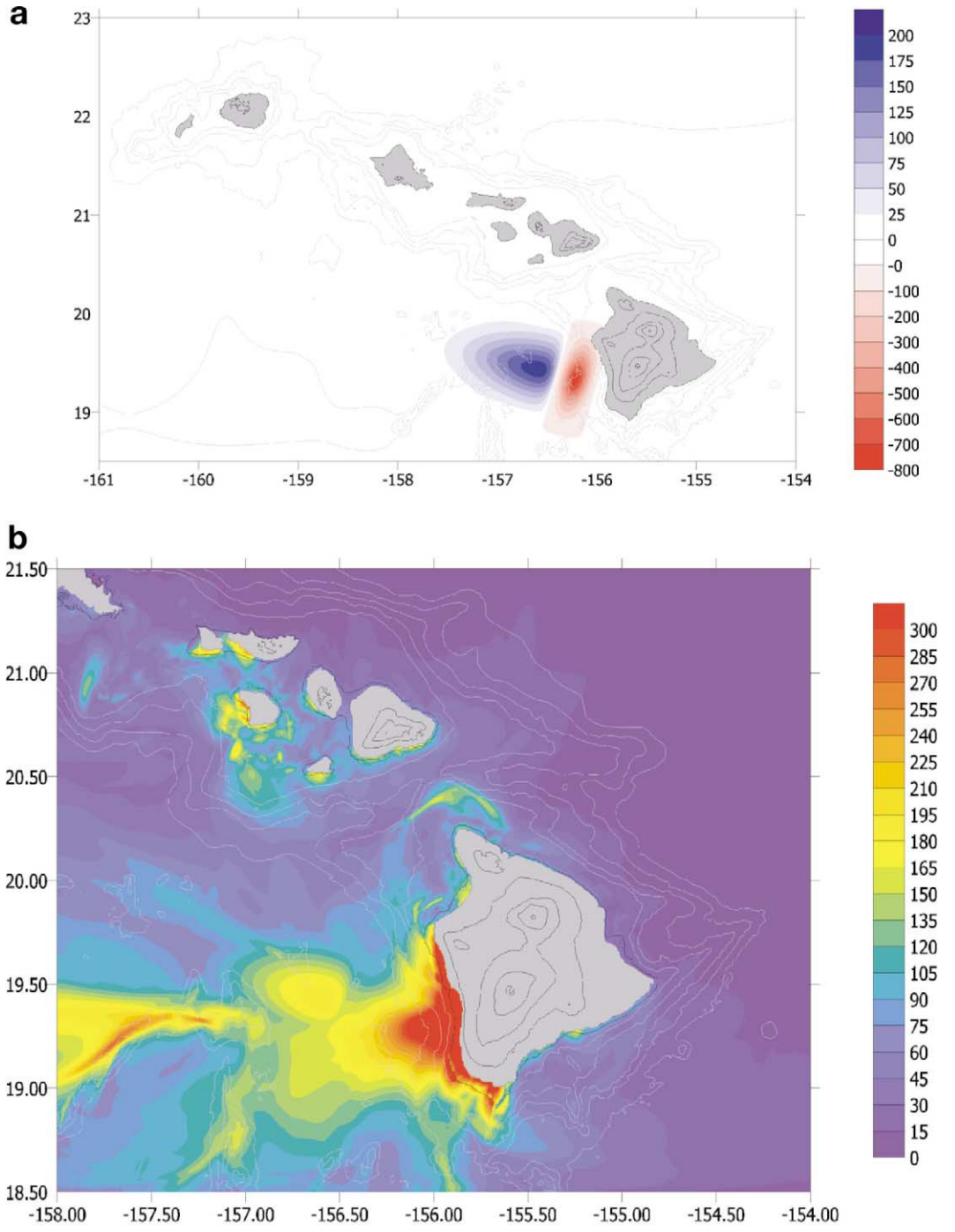
a
23
22
21
20
19
-161
-160
-159
-158
-157
-156
-155
-154
200
175
150
125
100
75
50
25
0
-0
-100
-200
-300
-400
-500
-600
-700
-800
b
21.50
21.00
20.50
20.00
19.50
19.00
18.50
-158.00
-157.50
-157.00
-156.50
-156.00
-155.50
-155.00
-154.50
-154.00
300
285
270
255
240
225
210
195
180
165
150
135
120
105
90
75
60
45
30
15
0

initial condition is only correct to within about a factor of two, which is much larger than the intrinsic error of the tsunami generation model (Watts et al., 2000). Nevertheless, this technique represents a significant improvement in accuracy over dipolar sources previously used to model Alika phase 2, e.g. Johnson and Mader (1994), with whom our tsunami amplitudes generally agree. A tsunami generation simulation that uses actual bathymetry and does not depth-average wave mechanics is still the subject of active research (Grilli and Watts, 2001; Grilli et al., 2002).

The 1998 Papua New Guinea (PNG) tsunami provides some perspective on the tsunami amplitudes predicted here. The PNG tsunami source was a 6-km$^3$ slump that traveled $\sim$1 km in water averaging 1400 m deep (Tappin et al., 2001). The nearest shoreline was devastated by waves averaging 10 m above sea level from a tsunami source of similar amplitude. By way of comparison, the volume of the Alika phase 2 event is nearly 100 times larger with a similar mean depth as the PNG event. To a first approximation, tsunami amplitude is proportional to landslide volume for events of similar mean depth (Watts and Grilli, 2003). With Alika 2 roughly a hundred times more massive than the PNG slump, it is therefore not surprising to find tsunami amplitudes approaching 1 km (i.e. a hundred times larger than the 10-m PNG tsunami). These arguments apply also to other GSLs, such as the enormous Nuuanu event off northeastern Oahu. Given a volume of 2000–3000 km$^3$ (Satake et al., 2002), the Nuuanu landslide may have generated a mega-tsunami limited in amplitude near the generation region by the depth of the ocean itself, a conjecture that is reinforced by Eq. 2. There should be no question as to the tsunamigenic potential of Hawaiian GSLs.

## 3. Tsunami propagation and inundation

We simulated tsunami propagation and inundation with the code TUNAMI-N2 (IUGG/IOC TIME Project, 1997). TUNAMI-N2 is a finite-difference code for solving the depth-averaged shallow-water wave equations; its design and stability are discussed by Imamura and Goto (1988). We used the latest available multibeam bathymetry gridded over a uniform cell spacing of 493 m. There remains significant uncertainty as to the subsidence history of individual islands, most of which differ and have not been monotonic since 125 ka BP (Wessel and Keating, 1994). Our simulation is therefore run for the present island elevations and consideration of subsidence history is made after the fact. Fig. 3b indicates that tsunami wave heights and runup would be highest along the western coast of Hawaii Island due to energy directivity (Iwasaki, 1997), with values $>$300 m extending from Keahole to Ka Lae (South Point; Fig. 1), in general agreement with Johnson and Mader (1994). Runup exceeds 750 m along 5 km of coastline, reaching a maximum of 803 m at Hookena (see Fig. 1 for location).

Other Hawaiian Island coastlines severely affected by this tsunami include the south and west shores of Maui, Kahoolawe, Lanai, Molokai, and Oahu (Fig. 3b). If coastlines were near their present locations, the isthmus between east and west Maui would be flooded, as well as low-lying portions of west Molokai and southwestern Oahu. The tsunami is focused onto Lanai by a shallow shelf south of the island. Some wave energy is reflected away from Lanai by this shelf even as the deeper water to the west guides the tsunami towards Lanai from the source. Interestingly, our results indicate that the maximum wave

Fig. 3. (a) Initial sea surface condition for the TUNAMI-N2 propagation code as provided by TOPICS 647 s after the initiation of Alika phase 2 giant landslide failure. Elevation and depression waves have different vertical scales. Contours are of present-day topography; the contour interval is 1000 m. The landslide was modeled with a head scarp coincident with the inferred present location of the Kealakekua fault at about 2000 m elevation landward of the slide (Fig. 1). (b) Maximum wave heights of the tsunami computed using TUNAMI-N2. Contours are of present-day topography; the contour interval is 1000 m. We find maximum runup consistent with the elevations of soil stripping, dated marine deposits, and previously conjectured tsunami amplitude amongst the Hawaiian Islands. Despite uncertainties in where sea level was, our modeling is approximately correct for Lanai, Molokai, and west Maui. As previously pointed out (Moore and Moore, 1988), we expect mainly erosion on the steep island slopes, although a mega-tsunami may deposit material along a thin high-water mark or in sheltered topography.

Table 1
Age estimates of Hawaiian giant submarine landslides

| GSL name | Source volcano | Estimated age range (Ma) | Estimated age method | Oxygen Isotope Stage[a] | Explanation | Reference |
|---|---|---|---|---|---|---|
| Hilina slump | Kilauea | >0.010–0.100 | Marine sediment stratigraphy; Volcanic flow stratigraphy | 1, 3? | Min. age estimate from lower $^{230}$Th dating limit of pelagic sed. over massive turbidites; max. age from estimated submarine–subaerial flow transition. | McMurtry, Herrero-Bervera and Kanamatsu (unpubl. data); Moore and Clague (1992) |
| Ka Lae East and West debris avalanches (2) | Mauna Loa | >0.032–0.060? | Volcanic flow stratigraphy | 3 | Acoustic images suggest ages younger than Alika; upper age limits from $^{14}$C dates of subaerial flows, assuming Kahuku fault is headwall. | Moore and Clague (1992); Lockwood (1995) |
| Punalu'u slump | Mauna Loa | 0.100–0.200 | Volcanic flow stratigraphy | 5, 7? | K–Ar age range of Ninole Basalt, in ML headwall. | Lipman (1995) |
| Alika phase 1 and 2 debris avalanches (2) | Mauna Loa | >0.112–0.127 | Marine sediment stratigraphy | 5 | Min. age from $^{230}$Th dating of pelagic sediment cover on turbidite; best (max.) age from $\delta^{18}$O of included foraminifera. | McMurtry et al. (1999) |
| North Kona slump | Hualalai | >0.130 | Shield apex | 5? | Age of transition from tholeiitic to alkalic volcanism. | Moore and Clague (1992) |
| South Kona slump | Mauna Loa | 0.200–0.240 | Marine sediment stratigraphy | 7 | Max. age from max. sediment thickness observed on slide block and lowest sed. rate measured in area. Ages agree with ML apex age (0.25 Ma). | Moore et al. (1995); McMurtry et al. (1999) |
| Pololu debris avalanche | Kohala | 0.254–0.306 | Volcanic flow stratigraphy | 9 | Min. age from oldest Hawi flows; max. age from youngest Pololu Basalt. | Moore and Clague (1992) |
| Hana debris avalanche | Haleakala | 0.86 | Shield apex | 25 | Max. K–Ar age of E. Maui flows (=apex?); at lower est. transition (apex) U-series age of 0.85 Ma (H coral terrace). | In Keating (1987); Moore and Clague (1992) |
| Wailau debris avalanche | E. Molokai | 1.0±0.1 | Marine sediment stratigraphy | 31 | Magnetostratigraphic age of turbidite in pelagic sediment capping Tuscaloosa Seamount (largest Nuuanu GSL block). | Kanamatsu et al. (2002) |
| Clarke debris avalanche | Lanai | 1.3±0.06 | Shield apex | 46? | Weighted mean of youngest, reliable Lanai shield flow ages ($n=6$). Magnetostratigraphic ages of flows indicate rapid eruption in Matuyama Polarity Chron. | Bonhommet et al. (1977); Herrero-Bervera et al. (2000) |
| Nuuanu debris avalanche | Koolau (NE Oahu) | 2.1–2.2 | Shield apex | 87? | Youngest Koolau shield flows, in agreement with recent rock magnetostratigraphy results. Pelagic sediment magnetostratigraphy indicates GSL age >1.8 Ma. | In Keating (1987); Herrero-Bervera et al. (2002); Kanamatsu et al. (2002) |

Table 1 (*Continued*).

| GSL name | Source volcano | Estimated age range (Ma) | Estimated age method | Oxygen Isotope Stage[a] | Explanation | Reference |
|---|---|---|---|---|---|---|
| Waianae slump | Waianae (SW Oahu) | 2.9–3.1 | Volcanic flow stratigraphy | - | Ages of postshield, alkalic Waianae flows and formation of Lualualei Valley. | Presley et al. (1997) |
| Kaena debris avalanche | Waianae (NW Oahu) | 3.6 | Shield apex | – | Probable apex age of NW Waianae shield flows (range is 2.9–3.9 Ma). | Presley et al. (1997) |
| Kauai, North and South debris avalanches (2) | Kauai | 5.0 | Shield apex | – | Probable apex age of Kauai shield; K–Ar radiometric ages range 3.8–5.3 Ma. | In Keating (1987) |
| Nihoa debris avalanches (3+?) | Nihoa | 7.0 (7.3)[b] | Shield apex | – | Mean age of shield flows ($n = 9$) | In Keating (1987) |
| Necker debris avalanches (2) | Necker | 11.7 (10.6) | Shield apex | – | Mean age of shield flows ($n = 7$) | In Keating (1987) |
| Gardner slumps (3) | Gardner Pinnacles | 12.3 (15.8) | Shield apex | – | Age of shield (?) flow ($n = 1$) | In Keating (1987) |
| Laysan, Maro slumps (3) | Laysan, Maro Reefs | 20.3 (19.7–20.7) | Shield apex | – | Mean age of shield (?) flows ($n = 13$) | In Keating (1987) |
| Pearl and Hermes debris avalanche | Pearl and Hermes Reefs | 20.1 (26.8) | Shield apex | – | Mean age of shield (?) flows ($n = 3$) | In Keating (1987) |
| Midway debris avalanches (2) | Midway | 28.6 (28.7) | Shield apex | – | Max. age = shield apex? | In Keating (1987) |

[a] Oxygen isotope stages from Joyce et al. (1990).
[b] Bracketed ages calculated from plate motion (Clague, 1996).

heights and runup for Lanai, greater than 300 m in elevation, are along the western coast, and not in the southern coastal areas studied by J. Moore and others (Moore and Moore, 1984, 1988; Grigg and Jones, 1997; Felton et al., 2000; Rubin et al., 2000). The discovery of deposits on southern Lanai has been ascribed to their preservation by drier conditions and to their relative shelter from erosion (Moore and Moore, 1988). In general, we find agreement between the debris locations and our simulation results, supporting the theory of mega-tsunami emplacement of the coral-bearing deposits and constraining the subsidence history of Lanai.

## 4. Island subsidence implications

A key problem with interpreting exposed deposits is the subsidence or emergence history of the different islands. The only island that has a well-known history is Hawaii, which has been

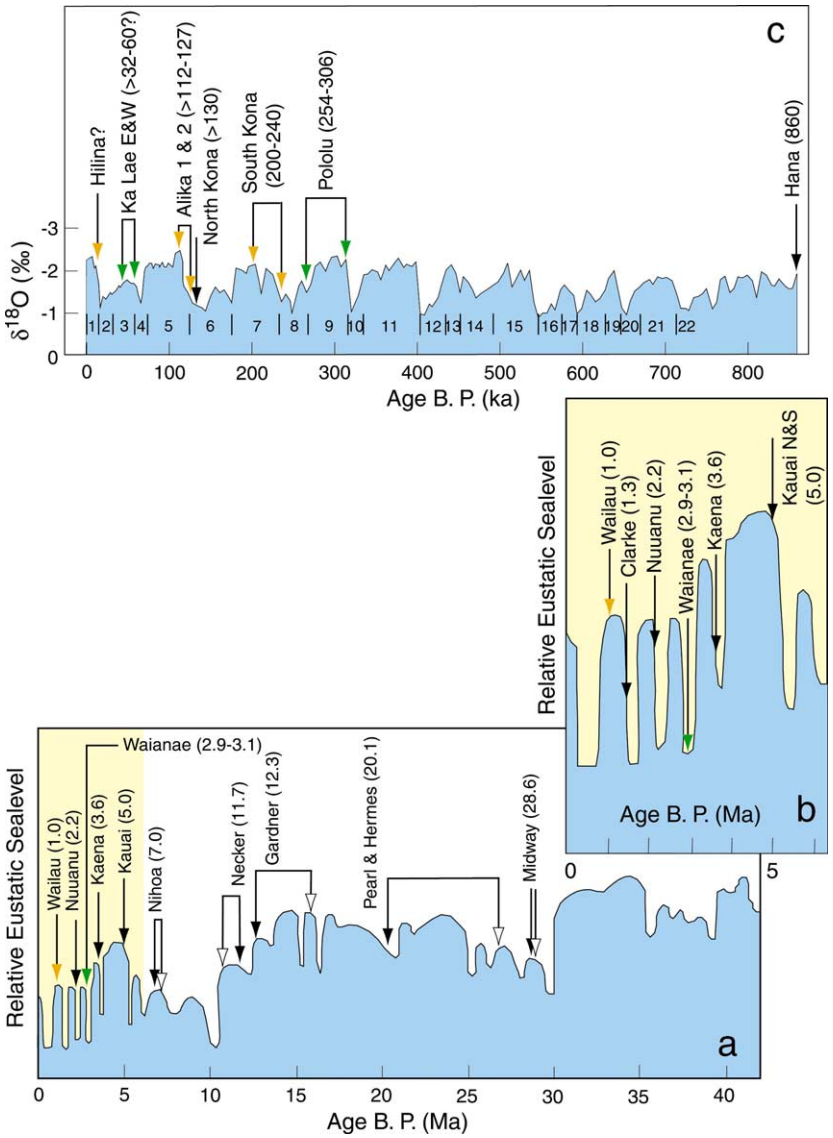

steadily subsiding for more than 475 ka. For Hawaii, the present coastline would have been at about 325 m elevation at ca. 125 ka BP, based upon a uniform subsidence rate of 2.6 mm/yr over the past 475 ka (Ludwig et al., 1991). This subsidence is small relative to the 2000 m altitude of the Kealakekua–Kahuku fault system, and it renders our tsunami source conservative. An in situ coral fragment found 6 m above sea level on the northwest Kohala coast of Hawaii was U-series dated at 110 ± 10 ka and was probably deposited by the Alika phase 2 mega-tsunami at > 330 m elevation based upon the aforementioned subsidence rate (Stearns, 1973; Moore and Moore, 1984). Recent work on the marine fossiliferous basalt-boulder conglomerates found on Kohala supports the ca. 100 ka age and extends the runup elevation there to > 430 m (McMurtry et al., 2002). Elevated marine deposits are still subject to interpretation for Oahu, Molokai, Lanai, and western Maui because these islands may have become static or emergent after an initial stage of submergence (Wessel, 1993; Wessel and Keating, 1994; Smith and Wessel, 2000). Island emergence is often documented by terraces that are wave cut during sea-level high stands. On Lanai, Molokai, and west Maui, there is a relative absence of wave-cut terraces at higher elevations, suggesting little emergence. The offsetting effects of island emergence to the northwest and subsidence to the southeast suggest that sea level is changing slowly around Lanai, a contention supported by the recognition of all major submarine terraces offshore (see Fig. 1; Campbell, 1986). Such a sea-level stasis has been identified for late Pleistocene Oahu (Szabo et al., 1994). Sea-level stasis would enable our simulation results to apply directly to these islands and may explain the agreement between predicted and observed deposits on Lanai. Our tsunami simulation results could guide future searches for other potential tsunami deposits.

## 5. Climate control of GSLs?

Having added to the evidence for a connection between Hawaiian GSLs, mega-tsunami generation and elevated tsunami deposits, we seek the underlying mechanism for the correlation of volcanic failure with the common factor of the onset of sea-level high stands, at least for the stage 5e

Fig. 4. (a) Relative eustatic sea-level curve based upon seismic stratigraphy from 0 to > 40 Ma (from Haq et al., 1988) with Hawaiian Ridge Volcano 'apex' ages (black arrows; see text and Table 1) or giant submarine landslide (GSL) age estimates (orange arrows, marine sediment stratigraphy; green arrows, volcanic flow stratigraphy) selected from sources listed in Table 1. Locations of named GSLs and corresponding shield volcanoes are found in Moore et al. (1994b). The Hilina slump GSL (Fig. 1) is a prediction from our model. New dating evidence from massive turbidites in sediment cores taken > 100 km SE of Hawaii suggests very young landslide events (Naka et al., 2000; Kanamatsu et al., 2002 and unpubl. data). For the Leeward Islands (Necker to Midway) there are difficulties in obtaining radiometric samples representative of the main shield stage for many of these edifices; we use calculated ages (open arrows) from Clague (1996) to illustrate the uncertainty. (b) Detail of eustatic sea-level curve from 0 to > 5 Ma. (c) Relative sea-level curve from 0 to 860 ka BP based upon oxygen isotope stratigraphy. Glacial (even number) and interglacial (odd number) stages are indicated out to stage 22 (from Shackleton and Opdyke, 1973). Stratigraphic excess $^{230}$Th dating of the Alika phase 2 GSL indicates a minimum age of 112 ± 15 ka with a best age, derived from $\delta^{18}$O of foraminifera included in its turbidite, of 127 ± 5 ka, coincident with the stage 5e interglacial (McMurtry et al., 1999). Observations from a 1992 DSV *Sea Cliff* submersible dive on one of the large detached blocks of the South Kona GSL (Fig. 1) found up to 0.5 m of sediment on the top (Moore et al., 1995), which places its maximum age of emplacement at about 240 ka, based on a minimum, porosity-corrected excess $^{230}$Th sedimentation rate of 1.3 ± 0.2 mm/kyr from nearby pelagic sediments (core B13 in Fig. 1; McMurtry et al., 1999). Moore et al. (1994b) estimated a regional sedimentation rate near the islands by assuming the landslide ages correspond to the end of shield building of the volcano from which they originated. Based on K–Ar ages of lava flows from the host volcano (Clague and Dalrymple, 1987) and a sediment thickness, determined by surface ship 3.5-kHz echo sounding from the tops of debris hummocks or blocks, a mean sediment accumulation rate of ~2.5 mm/kyr was estimated (Moore et al., 1994b) which is consistent with recent excess $^{230}$Th sediment dating of pelagic sediments off Oahu (McMurtry, Herrero-Bervera and Kanamatsu, unpubl. data). This rate and thickness yield an approximate emplacement age of the South Kona slide block of 200 ka, within stage 7. The age is consistent with our maximum estimate of 240 ka and with an extrapolated age of 240 ± 80 ka for a large basal turbidite sequence in core PC-01 (Fig. 1; McMurtry et al., 1999).

and 7 interglacials. The instability of subaerial landslides most often hinges on weak bedding and soil saturation (Turner and Schuster, 1996), both of which depend directly or indirectly on climate. We find an intriguing relationship between the timing of Hawaiian GSLs and high stands of the sea, a proxy for long-term climate (Table 1; Fig. 4). The compilation of age estimates for the Hawaiian GSLs vs. paleo-sea level shows that nearly all of the GSLs correlate with the onset of warm interglacial periods back to Kauai at 5.0 Ma. Few reliable radiometric age estimates are available before this time. The apparent correlation between GSLs and high stands is opposite to that proposed for triggering of GSLs along the continental margins, where lower sea level in glacial times has been proposed to destabilize sediments built up during the previous interglacial period (Nisbet and Piper, 1998). For oceanic islands, the mechanism of failure apparently is different.

The climate probably becomes warmer and wetter in Pacific subtropical regions during Quaternary interglacials regardless of latitude (e.g. Broecker, 1995; Peterson et al., 2000), increasing water retention by porous volcanoes. This climatic condition, with possible increased frequency and severity of tropical storms, favors the phreatomagmatic triggering of GSLs by increasing the probability of groundwater interaction with magma (McMurtry et al., 1999). Phreatomagmatic triggering thus should be added to the list of potential GSL mechanisms needed beyond normal magma injection and groundwater pressure (Iverson, 1995), such as large earthquakes (e.g. Lipman et al., 1988) and overpressure from rapidly heated, dike-confined groundwater (Elsworth and Day, 1999). This mechanism is especially compelling if drier periods allow shallow magma chambers to fill unabated because of less frequent rainfall. Therefore, volcanic flank failure is attributed in one way or another to increased retention of groundwater due to climate change, rather than as a direct response to sea-level change.

In early November 2000, a large storm dropped nearly 1 m of rain over the Island of Hawaii, an island that had been undergoing severe drought for the past several years. Recently, Cervelli et al. (2002) correlated the storm to an episode of aseismic slip along the Hilina fault system, which represents the headwall of the giant Hilina Slump along Kilauea Volcano's south flank (Fig. 1). Although Cervelli et al. (2002) determined that the average 5 cm *per day* slip rate was substantially less than that needed for catastrophic failure, they point out that this rate was far faster than the inferred decimeter per year rates for Kilauea's decollement, and that flank failure must represent accelerating slip. These new observations reinforce our hypothesis that such large failures may be triggered by changing climate and rainfall patterns.

## 6. Conclusions

Tsunami deposits and vertical island motions in Hawaii and likely elsewhere remain largely unresolved issues for future study. For the late Pleistocene, large volcanic failures and exposed marine deposits both correlate foremost with sea-level high stands, and in particular with the onset of interglacial conditions that are reflected in Hawaii by the apex ages of the low-stand fringing reefs. We have shown that such large volcanic failures inevitably generate mega-tsunamis, and we conclude that persistent climate effects during sea-level high stands eventually unleash large volcanic failures and mega-tsunamis amongst the Hawaiian Islands and perhaps all volcanically active oceanic islands, with invariable propagation toward the continental coasts. The time of greatest island volcanic landslide hazard may be now.

## Acknowledgements

The authors thank Fris Campbell, Simon Day, Craig Glenn, Emilio Herrero-Bervera, Fred Mackenzie, and David Tappin for helpful discussions as well as Ahmet C. Yalciner for modifications of TUNAMI-N2. Comments from Juan-Carlos Carracedo, David Piper, and an anonymous reviewer improved the paper. Partial funding for this work was provided by NASA, the State of Hawaii, SOEST, and Applied Fluids En-

gineering, Inc. This is SOEST Contribution No. 6123, HIGP Contribution No. 1295.

## References


Bonhommet, N., Beeson, M.H., Dalrymple, G.B., 1977. A contribution to the geochronology and petrology of the island of Lanai, Hawaii. Geol. Soc. Am. Bull. 88, 1282–1286.

Broecker, W.S., 1995. The Glacial World According to Wally. Eldigio Press, Columbia Univ., Palisades, NY, 318 pp.

Campbell, J.F., 1986. Subsidence rates for the southeastern Hawaiian Islands determined from submerged terraces. Geo-Mar. Lett. 6, 139–146.

Carracedo, J.C., 1999. Growth, structure, instability, and collapse of Canarian volcanoes and comparisons with Hawaiian volcanoes. J. Volcanol. Geotherm. Res. 94, 1–19.

Cervelli, P., Segall, P., Johnson, K., Lisowski, M., Miklius, A., 2002. Sudden aseismic fault slip on the south flank of Kilauea volcano. Nature 415, 1014–1018.

Clague, D.A., 1996. The growth and subsidence of the Hawaiian–Emperor volcanic chain. In: Keast, A., Miller, S.E. (Eds.), The Origin and Evolution of Pacific Island Biotas, New Guinea to Eastern Polynesia: Patterns and Processes. SPB Academic Publ., Amsterdam, pp. 35–50.

Clague, D.A., Dalrymple, G.B., 1987. The Hawaii–Emperor volcanic chain. In: Decker, R.W., Wright, T.L., Stauffer, P.H. (Eds.), Volcanism in Hawaii. U.S. Geol. Surv. Prof. Pap. 1350.

Dixon, J.E., Clague, D.A., Stolper, E.M., 1991. Degassing history of water, sulfur, and carbon in submarine lavas from Kilauea volcano, Hawaii. J. Geol. 99, 371–394.

Duennebier, T., Reed, T., HIGP Staff, 1994. Northwestern Hawaiian islands: Merged bathymetry and topography [1:4,000,000], Sheet #2. Hawaii Seafloor Atlas, Hawaii Institute of Geophysics and Planetology, Honolulu, HI.

Edgers, L., Karlsrud, K., 1982. Soil flows generated by submarine slides: Case studies and consequences. Nor. Geotech. Inst. Bull. 143, 1–11.

Elsworth, D., Day, S.J., 1999. Flank collapse triggered by intrusion: The Canarian and Cape Verde Archipelagos. J. Volcanol. Geotherm. Res. 94, 323–340.

Felton, E.A., Crook, K.A.W., Keating, B.H., 2000. The Hulopoe gravel, Lanai, Hawaii: New sedimentological data and their bearing on the 'giant wave' (mega-tsunami) emplacement hypothesis. Pure Appl. Geophys. 157, 1257–1284.

Fryer, G.J., Watts, P., 2002. The 1946 Aleutian tsunami in the far field: Inadequacy of an earthquake source, confirmation of a landslide, and implications for warning. Eos, Trans. Am. Geophys. Union, 83 (47), Fall Meeting Suppl., Abstract OS51A-0147.

Fryer, G.J., Watts, P., Pratson, L.F., 2004. Source of the great tsunami of 1 April 1946: A landslide in the upper Aleutian forearc. Mar. Geol. 203, *X-ref:* doi: 10.1016/S0025-3227(03)00305-0, this issue.

Garcia, M.O., 1996. Turbidites from slope failure on Hawaiian volcanoes. In: McGuire, W.J., et al. (Eds.), Volcano Instability on the Earth and Other Planets. Geol. Soc. London Spec. Publ. 110, 281–294.

Goldfinger, C., Kulm, L.D., McNeill, L.C., Watts, P., 2000. Super-scale failure of the Southern Oregon Cascadia margin. Pure Appl. Geophys. 157, 1189–1226.

Grigg, R.W., Jones, A.T., 1997. Uplift caused by lithospheric flexure in the Hawaiian Archipelago as revealed by elevated coral deposits. Mar. Geol. 141, 11–25.

Grilli, S.T., Watts, P., 1999. Modeling of waves generated by a moving submerged body: Applications to underwater landslides. Eng. Anal. Bound. Elem. 23, 645–656.

Grilli, S.T., Watts, P., 2001. Modeling of tsunami generation by an underwater landslide in a 3D numerical wave tank. Proc. 11th Offshore and Polar Engineering Conference, ISOPE01, Stavanger, 3, 132–139.

Grilli, S.T., Vogelman, S., Watts, P., 2002. Development of a 3D numerical wave tank for modeling tsunami generation by underwater landslides. Eng. Anal. Bound. Elem. 26, 301–313.

Haq, B.U., Hardenbol, J., Vail, P.R., 1988. Mesozoic and Cenozoic chronostratigraphy and cycles of sea-level change. In: Sea-Level Changes – An Integrated Approach. SEPM Spec. Publ. 42, 71–108.

Herrero-Bervera, E., Canon-Tapia, E., Walker, G.P.L., Guerrero-Garcia, J.C., 2002. The Nuuanu and Wailau giant landslides: Insights from paleomagnetic and anisotropy of magnetic susceptibility (AMS) studies. Phys. Earth Planet. Inter. 129, 83–98.

Herrero-Bervera, E., Vinuela, J.M., Valet, J.-P., 2000. Paleomagnetic study of the ages of lavas on the island of Lanai, Hawaii. J. Volcanol. Geotherm. Res. 104, 21–31.

Holcomb, R.T., Searle, R.C., 1991. Large landslides from oceanic volcanoes. Mar. Geotechnol. 10, 19–32.

Imamura, F., Goto, C., 1988. Truncation error in numerical tsunami simulation by the finite difference method. Coast. Eng. Jpn. 31, 245–263.

IUGG/IOC TIME Project, 1997. Numerical method of tsunami simulation with the leap-frog scheme. Intergovernmental Oceanographic Commission Manuals and Guides 35, UNESCO, Paris.

Iverson, R.M., 1995. Can magma-injection and groundwater forces cause massive landslides on Hawaiian volcanoes? J. Volcanol. Geotherm. Res. 66, 295–308.

Iwasaki, S., 1997. The wave forms and directivity of a tsunami generated by an earthquake and a landslide. Sci. Tsunami Hazards 15, 23–40.

Johnson, C., Mader, C.L., 1994. Modeling of the 105 ka Lanai tsunami. Sci. Tsunami Hazards 12, 33–38.

Joyce, J.E., Tjalsma, L.R.C., Prutzman, J.M., 1990. High-resolution planktonic stable isotope record and spectral analysis for the last 5.35 M.Y.: Ocean Drilling Program site 625 Northeast Gulf of Mexico. Paleoceanography 5, 507–529.

Kanamatsu, T., Herrero-Bervera, E., McMurtry, G.M., 2002. Magnetostratigraphy of deep-sea sediments from piston cores adjacent to the Hawaiian Islands: Implications for ages of turbidites derived from submarine landslides. In:

Takahashi, E., Lipman, P., Garcia, M., Naka, J., Aramaki, S. (Eds.), Hawaiian Volcanoes: Deep Underwater Perspectives. AGU Monograph 128, pp. 51–63.

Keating, B.H., 1987. Summary of Radiometric Ages from the Pacific. IOC Tech. Ser. 32, Unesco, Paris.

Keating, B.H., Helsley, C.E., 2002. The ancient shorelines of Lanai, Hawaii, revisited. Sediment. Geol. 150, 3–15.

Kinoshita, W.T., Krivoy, H.L., Mabey, D.R., MacDonald, R.R., 1963. Gravity Survey of the Island of Hawaii. U.S. Geol. Survey Prof. Paper 475-C, pp. C114–C116.

Lènat, J.-F., Vincent, P., Bachèlery, P., 1989. The off-shore continuation of an active basaltic volcano: Piton de la Fournaise (Reunion Island, Indian Ocean); Structural and geomorphological interpretation of SeaBeam mapping. J. Volcanol. Geotherm. Res. 36, 1–36.

Lipman, P.W., 1995. Declining growth of Mauna Loa during the last 100,000 years: Rates of lava accumulation vs. gravitational subsidence. In: Rhodes, J.M., Lockwood, J.P. (Eds.), Mauna Loa Revealed: Structure, Composition, History, and Hazards. Am. Geophys. Union Monogr. 92, 45–80.

Lipman, P.W., Normark, W.R., Moore, J.G., Wilson, J.B., Gutmacher, C., 1988. The giant submarine Alika debris slide, Mauna Loa, Hawaii. J. Geophys. Res. 93, 4279–4299.

Lockwood, J.P., 1995. Mauna Loa eruptive history – the preliminary radiocarbon record. In: Rhodes, J.M., Lockwood, J.P. (Eds.), Mauna Loa Revealed: Structure, Composition, History, and Hazards. Am. Geophys. Union Monogr. 92, 81–94.

Ludwig, K.R., Szabo, B.J., Moore, J.G., Simmons, K.R., 1991. Crustal subsidence rate off Hawaii determined from 234U/238U ages of drowned coral reefs. Geology 19, 171–174.

McMurtry, G.M., Herrero-Bervera, E., Cremer, M., Resig, J., Sherman, C., Smith, J.R., Torresan, M.E., 1999. Stratigraphic constraints on the timing and emplacement of the Alika 2 giant Hawaiian submarine landslide. J. Volcanol. Geotherm. Res. 94, 35–58.

McMurtry, G.M., Tappin, D.R., Fryer, G.J., Watts, P., 2002. Megatsunami deposits on the Island of Hawaii: Implications for the origin of similar deposits in Hawaii and confirmation of the giant wave hypothesis. Eos, Trans. Am. Geophys. Union, 83 (47), Fall Meeting Suppl., Abstract OS51A-0148.

Moore, J.G., Clague, D.A., 1992. Volcano growth and evolution of the island of Hawaii. Geol. Soc. Am. Bull. 104, 1471–1484.

Moore, J.G., Moore, G.W., 1984. Deposit from a giant wave on the island of Lanai, Hawaii. Science 226, 1312–1315.

Moore, G.W., Moore, J.G., 1988. Large-scale bedforms in boulder gravel produced by giant waves in Hawaii. In: Sedimentologic Consequences of Convulsive Geologic Events. Spec. Pap. Geol. Soc. Am. 229, 101–110.

Moore, J.G., Clague, D.A., Holcomb, R.T., Lipman, P.W., Normark, W.R., Torresan, M.E., 1989. Prodigious submarine landslides on the Hawaiian Ridge. J. Geophys. Res. 94, 17465–17484.

Moore, J.G., Bryan, W.B., Ludwig, K.R., 1994a. Chaotic deposition by a giant wave, Molokai, Hawaii. Geol. Soc. Am. Bull. 106, 962–967.

Moore, J.G., Normark, W.R., Holcomb, R.T., 1994b. Giant Hawaiian landslides. Ann. Rev. Earth Planet. Sci. 22, 119–144.

Moore, J.G., Bryan, W.B., Beeson, M.H., Normark, W.R., 1995. Giant blocks in the South Kona landslide, Hawaii. Geology 23, 125–128.

Murty, T.S., 1979. Submarine slide-generated water waves in Kitimat Inlet, British Columbia. J. Geophys. Res. 84, 7777–7779.

Naka, J., et al., 2000. Tectono-Magmatic Processes Investigated at Deep-Water Flanks of Hawaiian Volcanoes. Eos, Trans. Am. Geophys. Union 81, 221, pp. 226–227.

Nisbet, E.G., Piper, D.J.W., 1998. Giant submarine landslides. Nature 392, 329–330.

Peterson, L.C., Haug, G.H., Huggen, K.A., Röhl, U., 2000. Rapid changes in the hydrologic cycle of the tropical Atlantic during the last glacial. Science 290, 1947–1951.

Presley, T.K., Sinton, J.M., Pringle, M., Postshield, 1997. Volcanism and catastrophic mass wasting of the Waianae Volcano, Oahu, Hawaii. Bull. Volcanol. 58, 597–616.

Raichlen, F., Lee, J.J., Petroff, C.M., Watts, P., 1996. The generation of waves by a landslide: Skagway, Alaska case study. Proc. 25th Int. Conf. Coastal Eng., Orlando, FL, ASCE, pp. 1293–1300.

Rubin, K.H., Fletcher, C.H., III, Sherman, C., 2000. Fossiliferous Lanai deposits formed by multiple events rather than a single giant tsunami. Nature 408, 675–681.

Ryan, M.P., 1988. The mechanics and three-dimensional internal structure of active magmatic systems: Kilauea Volcano, Hawaii. J. Geophys. Res. 93, 4213–4248.

Satake, K., Smith, J.R., Shinozaki, K., 2002. Three-dimensional reconstruction and tsunami model of the Nuuanu and Wailau giant landslides. In: Takahashi, E., Lipman, P., Garcia, M., Naka, J., Aramaki, S. (Eds.), Hawaiian Volcanoes: Deep Underwater Perspectives. AGU Monograph 128, 333–346.

Shackleton, N.J., Opdyke, N.D., 1973. Oxygen isotope and paleomagnetic stratigraphy of equatorial Pacific core V28–238: Oxyen isotope temperatures and ice volumes on a $10^5$ year and $10^6$ year scale. Quat. Res. 3, 39–55.

Smith, J.R., 1994. Island of Hawaii and Loihi submarine volcano, high resolution multibeam bathymetry around the Island of Hawaii, [1:75,000, 1:250,000, 1:500,000], Sheet #6. Hawaii Seafloor Atlas, Hawaii Institute of Geophysics and Planetology, Honolulu, HI.

Smith, J.R., Wessel, P., 2000. Isostatic consequences of giant landslides on the Hawaiian Ridge. Pure Appl. Geophys. 157, 1097–1114.

Stearns, H.T., 1973. Potassium-argon ages of lavas from the Hawi and Pololu volcanic series, Kohala Volcano, Hawaii: Discussion. Geol. Soc. Am. Bull. 84, 3483–3484.

Szabo, B.J., Ludwig, K.R., Muhs, D.R., Simmons, K.R., 1994. Thorium-230 ages of corals and the duration of the last interglacial sea-level high stand on O'ahu, Hawaii. Science 266, 93–96.

Tappin, D.R., Watts, P., McMurtry, G.M., Lafoy, Y., Matsumoto, T., 2001. The Sissano, Papua New Guinea tsunami of July 1998 – Offshore evidence on the source mechanism. Mar. Geol. 175, 1–23.

Tinti, S., Bortolucci, E., 2000. Energy of water waves induced by submarine landslides. Pure Appl. Geophys. 157, 281–318.

Turner, A.K., Schuster, R.L., 1996. Landslides: Investigation and Mitigation. Trans. Res. Board Spec. Rep. 247, National Academy Press, Washington, DC.

Watts, P., 1998. Wavemaker curves for tsunamis generated by underwater landslides. J. Waterw. Port. C-ASCE 124, 127–137.

Watts, P., 2000. Tsunami features of solid block underwater landslides. J. Waterw. Port. C-ASCE 126, 144–152.

Watts, P., Grilli, S.T., 2003. Underwater landslide shape, motion, deformation, and tsunami generation. Proc. 12th Offshore and Polar Eng. Conf., ISOPE03, Honolulu, Hawaii, HI, 3, pp. 364–371.

Watts, P., Imamura, F., Grilli, S.T., 2000. Comparing model simulations of three benchmark tsunami generation cases. Sci. Tsunami Hazards 18, 107–124.

Watts, P., Grilli, S.T., Kirby, J.T., Fryer, G.J., Tappin, D.R., 2003. Landslide tsunami case studies using a Boussinesq model and a fully nonlinear tsunami generation model. Nat. Hazards Earth Syst. Sci. 3, 391–402.

Wessel, P., 1993. A reexamination of the flexural deformation beneath the Hawaiian Islands. J. Geophys. Res. 87, 12177–12190.

Wessel, P., Keating, B.H., 1994. Temporal variations of flexural deformation in Hawaii. J. Geophys. Res. 99, 2747–2756.